Supporting Information

Homogeneous Adsorption of Multiple Potassiation Products of Red Phosphorus Anode towards Stable Potassium Storage

Feiyue Wang[a], Tong Yang[a], Wencong Feng[a], Jingke Ren[a], Xingbao Chen[a], Chaojie Cheng[a], Wen Luo[b,*], Xiaobin Liao[a,*], Liqiang Mai[a,*]

[a] *State Key Laboratory of Advanced Technology for Materials Synthesis and Processing, School of Materials Science and Engineering, Wuhan University of Technology, Wuhan 430070, P. R. China*

[b] *Department of Physics, School of Science, Wuhan University of Technology, Wuhan 430070, P. R. China*

*** Corresponding authors.**

Wen Luo — *Department of Physics, School of Science, Wuhan University of Technology, Wuhan 430070, P. R. China; orcid.org/0000-0002-1732-295X; E-mail: luowen_1991@whut.edu.cn*

Xiaobin Liao — *State Key Laboratory of Advanced Technology for Materials Synthesis and Processing, School of Materials Science and Engineering, Wuhan University of Technology, Wuhan 430070, P. R. China; orcid.org/0000-0002-2455-832X; E-mail: liaoxiaobin@live.com*

Liqiang Mai — *State Key Laboratory of Advanced Technology for Materials Synthesis and Processing, School of Materials Science and Engineering, Wuhan University of Technology, Wuhan 430070, P. R. China; orcid.org/0000-0003-4259-7725; E-mail: mlq518@whut.edu.cn*

Table S1. Detailed results of EIS analysis.

Materials	R_s（Ω）	R_{ct}（Ω）
RP/C	77.4	8284
NiPc@RP/C	64.7	7804
FePc@RP/C	18.5	5087
CoPc@RP/C	16.2	6087

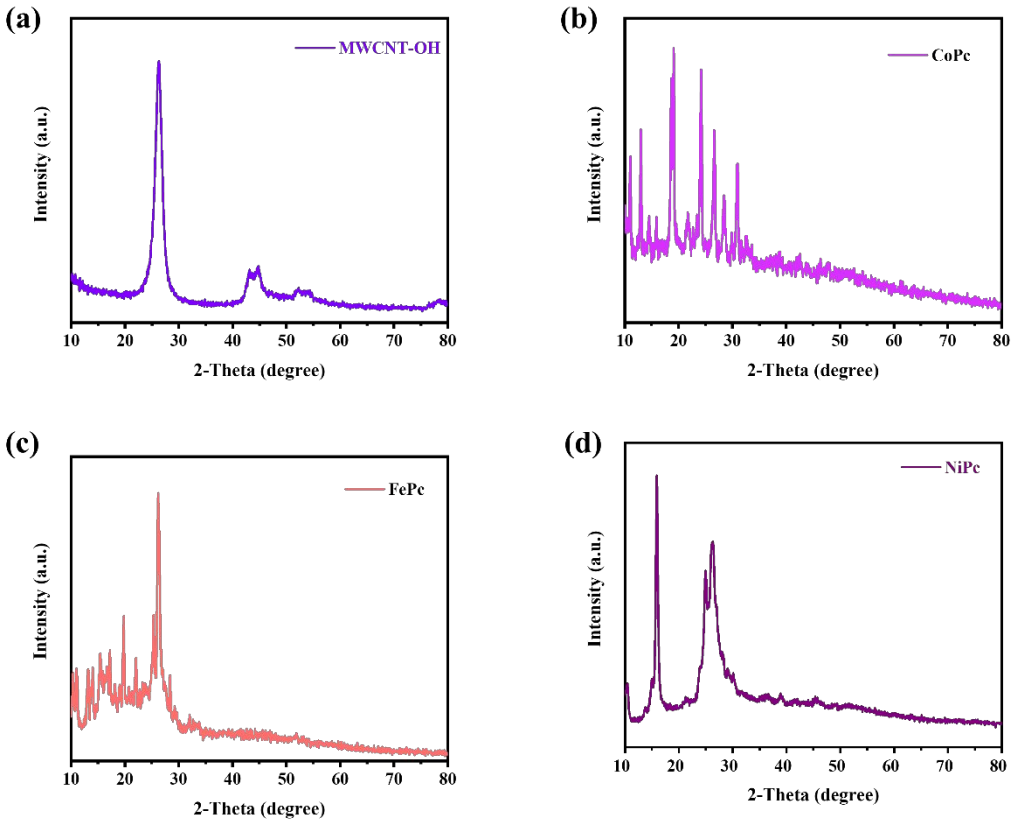

Figure S1. (a) XRD pattern of MWCNT-OH; (b) XRD pattern of CoPc; (c) XRD

pattern of FePc; (d) XRD pattern of NiPc.

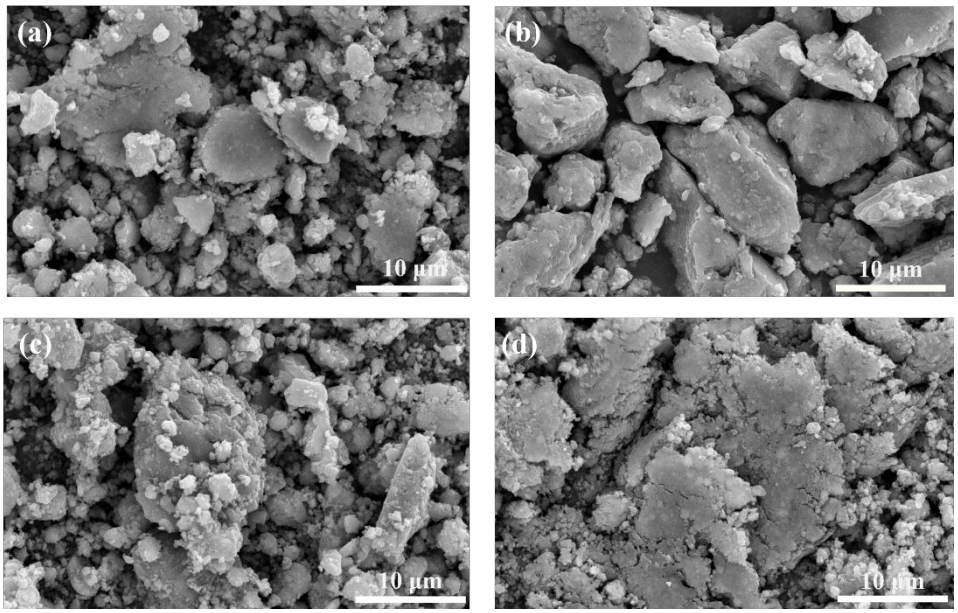

Figure S2. (a) SEM image of CoPc@RP/C; (b) SEM image of FePc@RP/C; (c) SEM image of NiPc@RP/C; (d) SEM image of RP/C.

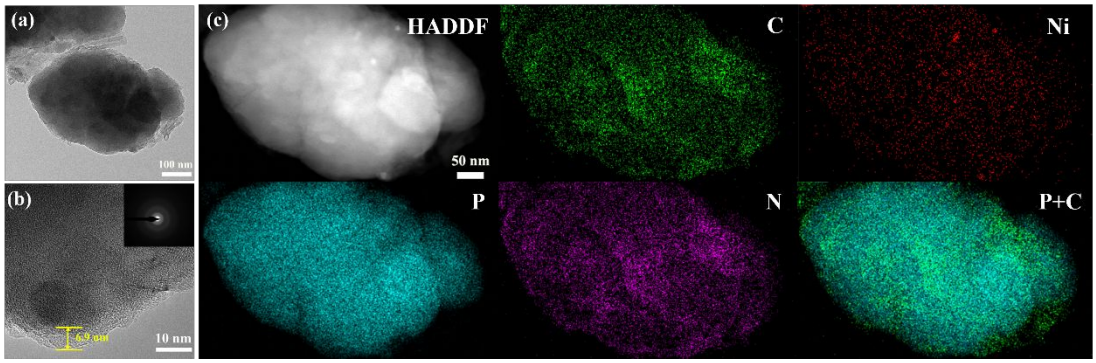

Figure S3. (a) TEM image of NiPc@RP/C; (b) HRTEM image of NiPc@RP/C (inset: the SAED pattern); (c) EDS elemental mapping of NiPc@RP/C.

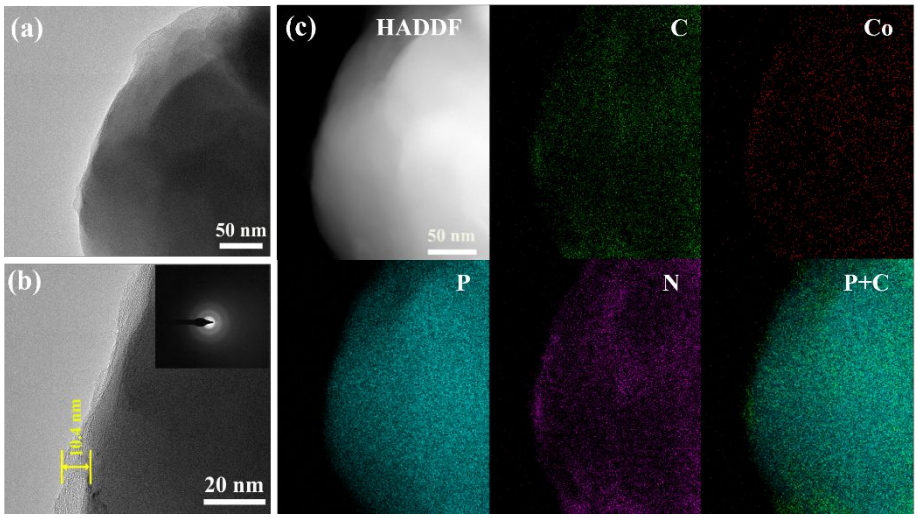

Figure S4. (a) TEM image of CoPc@RP/C; (b) HRTEM image of CoPc@RP/C (inset: the SAED pattern); (c) EDS elemental mapping of CoPc@RP/C.

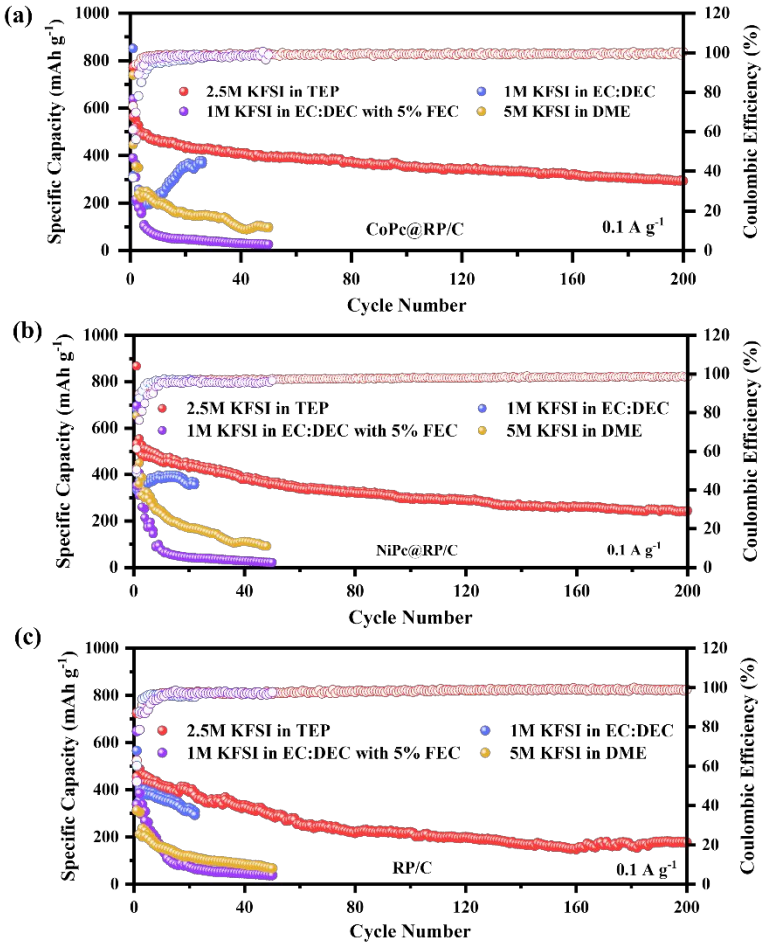

Figure S5. (a)~(c) Cycling performance of CoPc@RP/C, NiPc@RP/C and RP/C with

different electrolytes at a current density of 0.1 A g^{-1}, respectively.

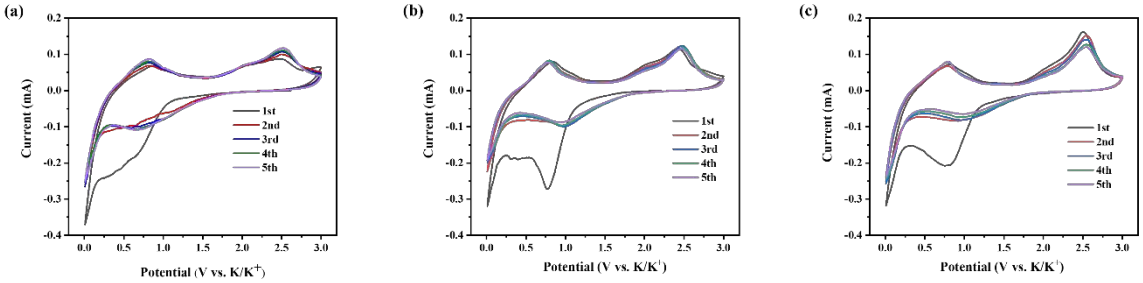

Figure S6. (a) CV curves at 0.2 mV s^{-1} scan rate of CoPc@RP/C; (b) CV curves at 0.2 mV s^{-1} scan rate of NiPc@RP/C; (c) CV curves at 0.2 mV s^{-1} scan rate of RP/C.

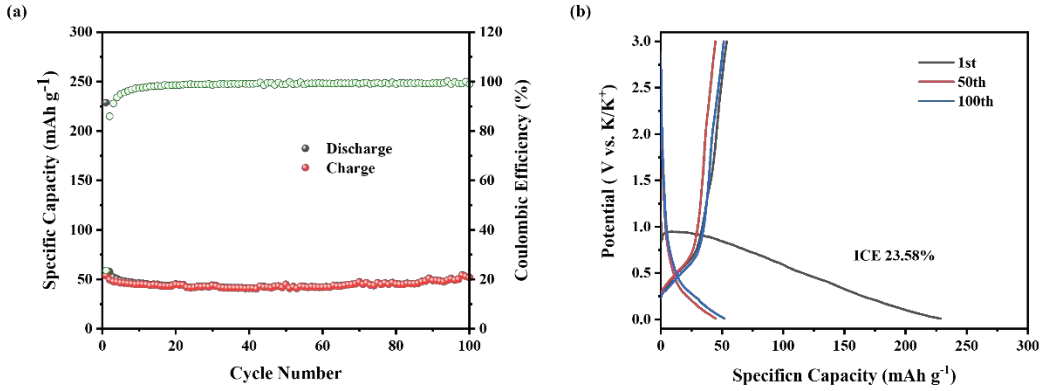

Figure S7. (a) Cycling performance of graphitized hydroxylated multi-walled carbon nanotubes at 0.1 A g^{-1}; (b) Charge-discharge curves of graphitized hydroxylated multi-walled carbon nanotubes at 0.1 A g^{-1}.

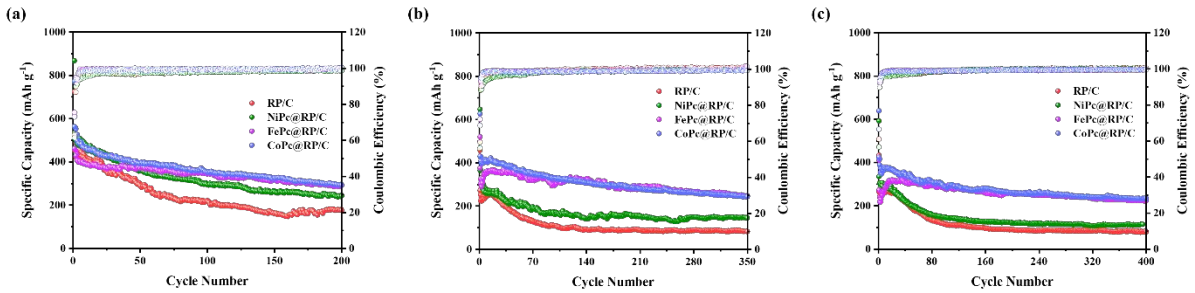

Figure S8. (a)~(c) Cycling performance at 0.1 A g^{-1}, 0.2 A g^{-1} and 0.3 A g^{-1} current densities of MPc@RP/C and RP/C.

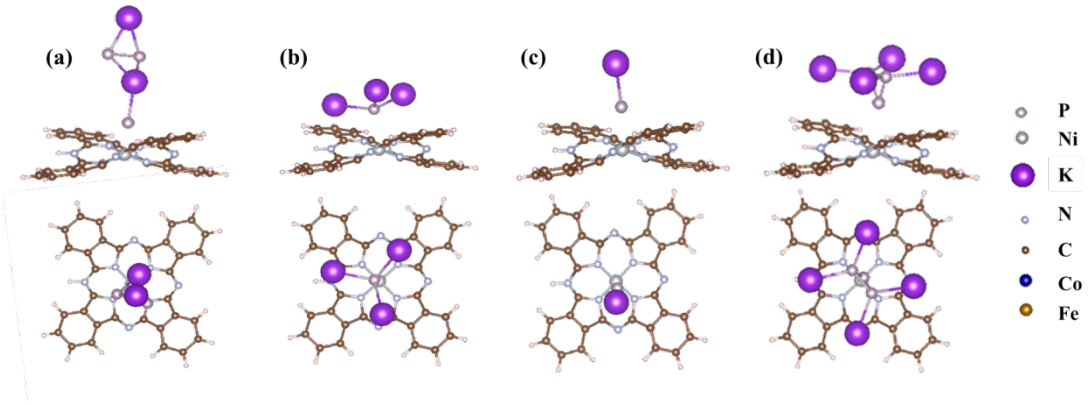

Figure S9. (a)~(d) Modeling the adsorption of K_2P_3, K_3P, KP,and K_4P_3 on NiPc, respectively.

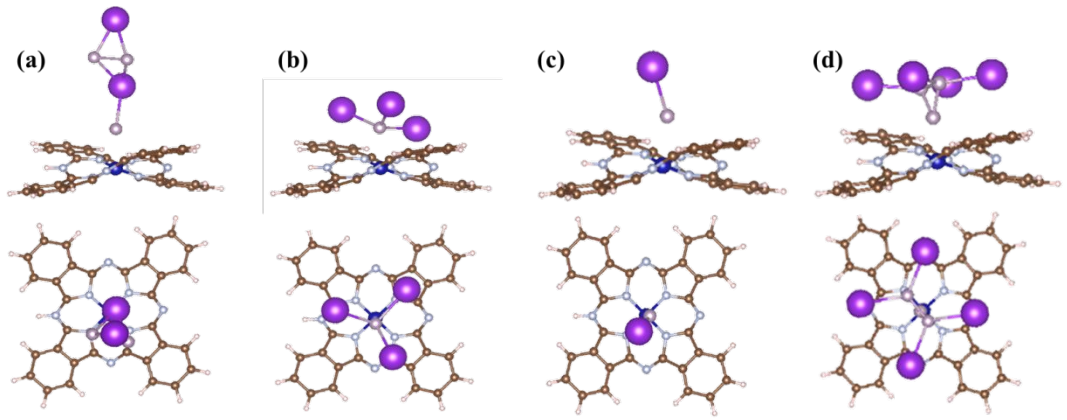

Figure S10. (a)~(d) Modeling the adsorption of K_2P_3, K_3P, KP,and K_4P_3 on CoPc, respectively.

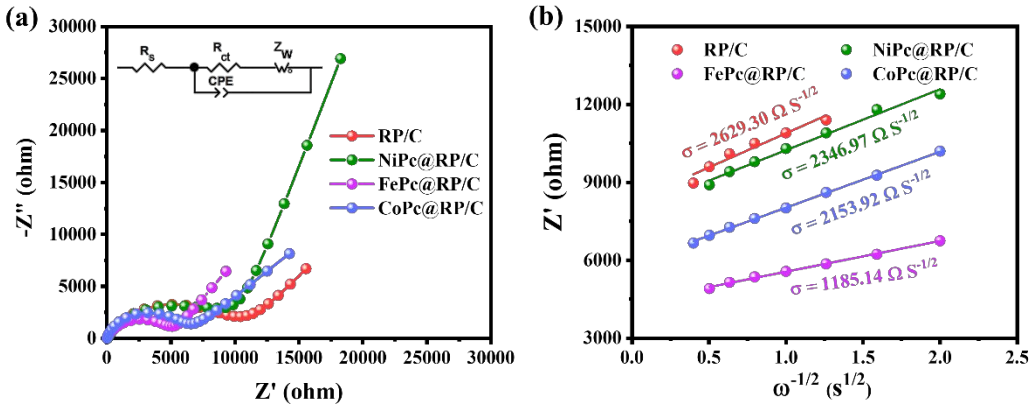

Figure S11. (a) electrochemical impedance profile fitted using the Randles equivalent circuit model (inset); (b) linear fit of Z′to $\omega^{-1/2}$ ($\omega = 2\pi f$) in the low-frequency region.

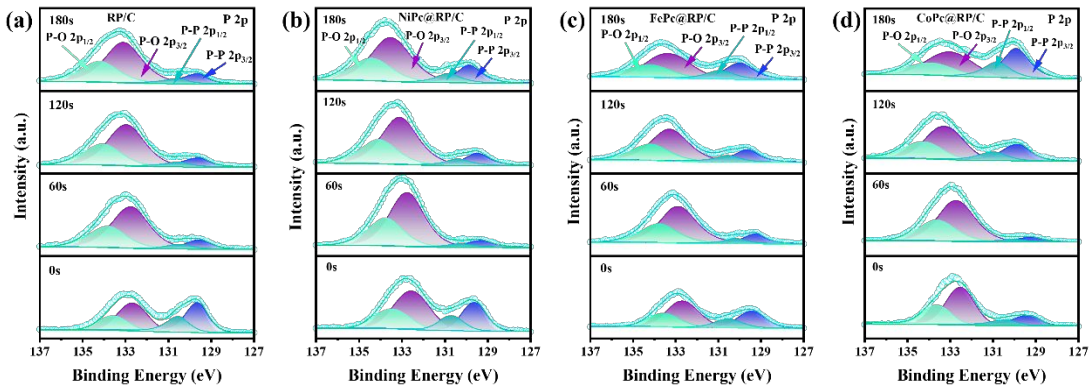

Figure S12. (a)~(d) P 2p spectras of XPS depth profile analysis for RP/C, NiPc@RP/C, FePc@RP/C and CoPc@RP/C after 10 cycles, respectively.

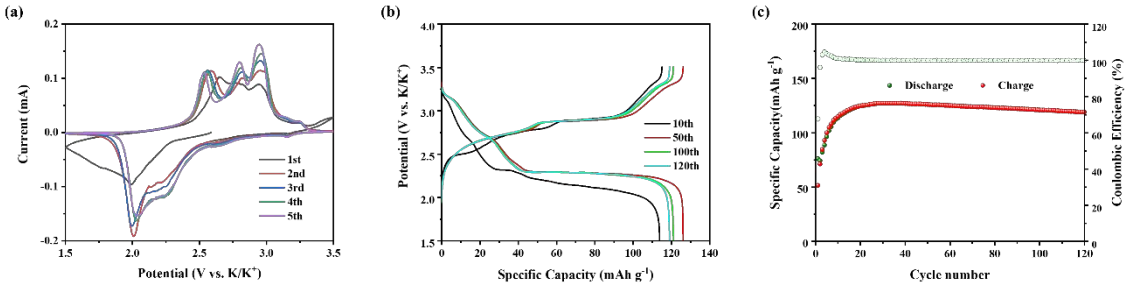

Figure S13. (a) CV curves of PTCDA potassium half cell at a scan rate of 0.1 mV s^{-1}; (b) Charge-discharge curves of PTCDA potassium half cell at 0.1 A g^{-1}; (c) Cycling performance of PTCDA potassium half cell at 0.1 A g^{-1}.

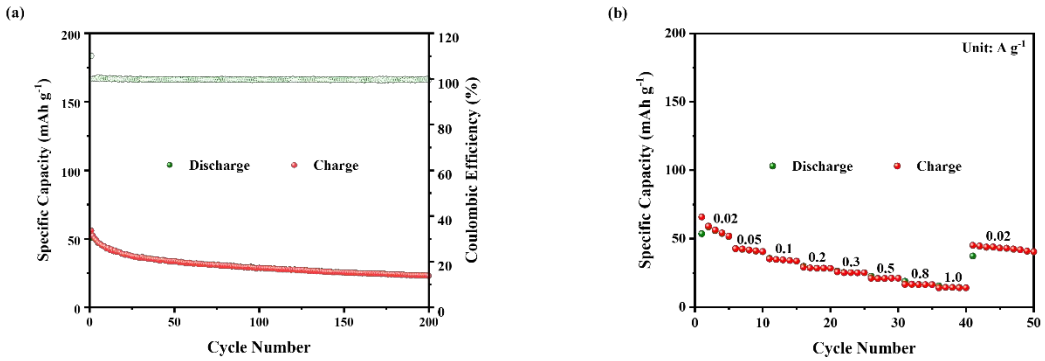

Figure S14. (a) Cycling performance of PTCDA//NiPc@RP/C full cell at 0.1 A g^{-1}; (b) Rate performance of PTCDA//NiPc@RP/C full cell at different current densities.

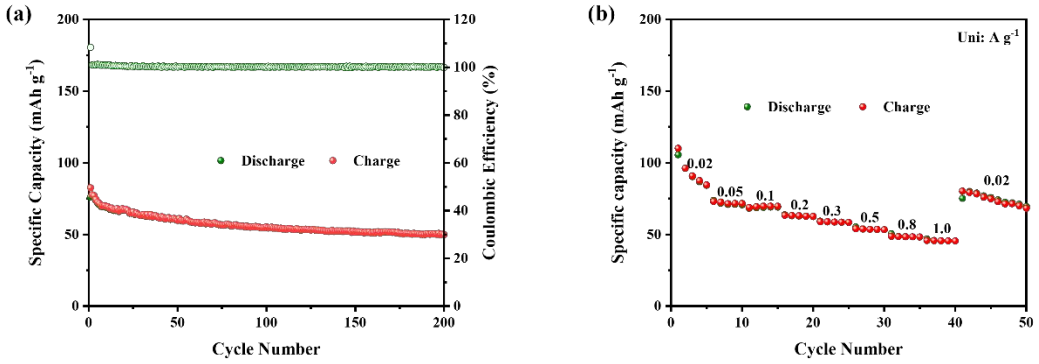

Figure S15. (a) Cycling performance of PTCDA//CoPc@RP/C full cell at 0.1 A g^{-1}; (b) Rate performance of PTCDA//CoPc@RP/C full cell at different current densities.